ANALYSIS OF GaAs MESFET SPECTRUM REGENERATION DRIVEN BY A π/4-DQPSK MODULATED SOURCE

John F. Sevic*, *Member IEEE*, Michael B. Steer**, *Senior Member IEEE*

*Motorola CSPD, Phoenix, AZ (602)244-6901
**North Carolina State University, Raleigh, NC (919)515-5191

ABSTRACT

A new method of analyzing transistor nonlinearity in the context of digital modulation is proposed. Classical methods of nonlinearity analysis, such as the third-order intercept point, are ill-suited for systems based on digitally modulated signals. The third-order intercept point ignores higher-order effects and latent out-of-channel power, both of which affect spectrum regeneration. Using a power spectral density description of the source, coupled with a simplified Volterra series model of a GaAs MESFET, it is shown that reactive nonlinearity significantly contributes to spectrum regeneration. Subsequently, insight is gained at the device level for doping/implant improvements and at the terminal level for optimal loading, resulting in improved linearity.

I. INTRODUCTION

Present and future wireless communication systems rely almost exclusively on digital modulation, with many digital cellular systems adopting some form of QPSK-based format [1]. Digital modulation in general, and the π/4-DQPSK format in particular, are fundamentally different from analog modulation in that the resultant spectrum is generally continuous [2]. Consequently, transistor nonlinearity characterization by the third-order intercept point is inappropriate: nonlinearity must alternatively be characterized by the ratio of total power over one frequency continuum to the total power of a neighboring continuum [3]. The third-order intercept point method ignores higher-order effects and latent out-of-channel power (a function of the peak-to-average ratio of the modulating signal), both of which affect directly aggregate spectrum regeneration. Each of these effects must be considered to assess their individual impact on spectrum regeneration.

Classical transistor nonlinearity characterization, based on the third-order intercept point, is usually limited to two-tone excitation. However, digitally modulated signals, and the resultant spectrum regeneration, must be described by a power spectral density. To analyze spectrum regeneration and identify which transistor nonlinearities are most significant, a new method of analyzing nonlinearity is proposed. The new method couples a power spectral density description of the excitation with a Volterra series model of transistor nonlinearity [4]-[6]. To demonstrate its usefulness, the method is used analyze each of the four predominate nonlinearities contributing to spectrum regeneration in a GaAs MESFET driven by a π/4-DQPSK source.

II. NONLINEAR MODEL OF GaAs MESFET AND MODEL EXTRACTION

Consider the simplified extrinsic MESFET equivalent circuit in Figure 1, where it is convenient to consider the port currents as a function of the port voltages. Each terminal current may be expressed as a sum of constituent currents: drift current, displacement current, and avalanche current. In the absence of breakdown, the port currents consist of drift current and displacement current only, and are in general nonlinear functions represented as

$$i_{drift} = g(v_{gs}, v_{ds}, \omega) \quad (1)$$

$$i_{disp} = j\omega \cdot h(v_{gs}, v_{ds}, \omega) \quad (2)$$

where ω is the radian frequency and the time derivative operator has been replaced by the $j\omega$ operator for assumed steady state. Four nonlinearities are independently considered. The drift current term (1) consists of the nonlinear transconductance and nonlinear output conductance. The displacement current term (2) consists of nonlinear depletion capacitances arising from the gate-channel junction. Output capacitance and transit-time are assumed independent of the port voltages.

The method of nonlinear currents based on third-degree Taylor expansions was used to derive Volterra nonlinear transfer functions up to third-order for the equivalent MESFET circuit of Figure 1 [7]. Consideration of only one nonlinearity per analysis simplified generation of the Volterra nonlinear transfer functions, which were derived in closed-form using Mathematica [8]. Taylor expansions representing the constituent currents of (1) and (2) are expressed as

$$i_{drift,gm} = g_{m1}v_{gs} + g_{m2}v_{gs}^2 + g_{m3}v_{gs}^3 \quad (3)$$

$$i_{drift,gds} = g_{ds1}v_{ds} + g_{ds2}v_{ds}^2 + g_{ds3}v_{ds}^3 \quad (4)$$

$$i_{disp,Cgs} = j\omega \cdot (C_{gs1}v_{gs} + C_{gs2}v_{gs}^2 + C_{gs3}v_{gs}^3) \quad (5)$$

$$i_{disp,Cgd} = j\omega \cdot (C_{gd1}v_{gd} + C_{gd2}v_{gd}^2 + C_{gd3}v_{gd}^3) \quad (6)$$

where cross-terms are assumed negligible. The device used in the analysis was a 400 μm x 1.0 μm Motorola CS-1 GaAs MESFET biased at 6.0 V and 30 mA ($0.5I_{dss}$). Coefficients for (3) - (6) were extracted at 850 MHz and $P_{out}/P_{1\,dB}$ = -7.0 dB using least-squares fits to measured data from an HP 8510C network analyzer. The accuracy of the extraction was verified using Symbolically Defined Devices in the HP MDS to simulate the equivalent circuit of Figure 1 [9]. Measured and simulated two-tone intermodulation distortion was found to be in excellent agreement at the frequency and power level extracted.

III. ANALYSIS AND RESULTS

The excitation source is described by a power spectral density following the North American Digital Cellular standard, with the modification that the receive root-raised cosine filter was not included in the integrations described next [1]. The power in the main channel over a 30 kHz BW, in terms of the input power spectral density *S(f)*, is

$$P_m = \int_{f_o-15\text{kHz}}^{f_o+15\text{kHz}} |H_1(f)|^2 S(f)\,df \quad (7)$$

where it has been assumed that the power present in the main channel is due to linear terms only. The upper adjacent-channel power, in terms of the input power spectral density *S(f)*, is

$$P_a = \int_{f_o-15\text{kHz}}^{f_o+15\text{kHz}} |H_3(f,\alpha,T_s)|^2 S(f) **df \quad (8)$$

where α and T_s are modulation constants and "**" denotes double convolution of *S(f)* with itself. In (7) and (8), H_1 and H_3 represent first- and third-order Volterra nonlinear transfer functions, respectively, based on (3)-(6).

The individual contribution of each nonlinearity (3)-(6) to spectrum regeneration was analyzed by simultaneously linearizing the remaining three nonlinearities of the equivalent circuit of Figure 1. The results are shown in Table 1 below. The ratio of P_a to P_m is defined as the adjacent-channel power ratio; a ratio of -50 dBc would represent an ideal amplifier. Figures 2 through 5 shows the simulated spectrum regeneration for nonlinear transconductance, gate-source depletion capacitance, gate-drain depletion capacitance, and output conductance, respectively.

From the results it is clear that nonlinear transconductance is the most significant contributor to spectrum regeneration. It

should be noted that both second- and third-degree nonlinearities influence adjacent-channel spectrum regeneration. The next most predominant term was nonlinear gate-source depletion capacitance. Similarly, both second- and third-degree nonlinearities influence adjacent-channel spectrum regeneration. The remaining two nonlinearities, the gate-drain depletion capacitance and the output conductance, made relatively small contributions to spectrum regeneration.

IV. CONCLUSION

A new method of analyzing transistor nonlinearity in the context of digital modulation was presented. The method, based on a power spectral density description of the source coupled with a Volterra series transistor model, provides device level insight for nonlinearity analysis that a simplified third-order intercept analysis does not. The method was used to determine the predominant nonlinearities of a GaAs MESFET, demonstrating that reactive nonlinearity is significant. Planned future work will consider generation of the Volterra nonlinear transfer functions with a harmonic-balance simulator, facilitating analysis of multiple simultaneous nonlinearities. The method presented here should find application in device level linearity improvement, development of optimal source/load impedances for best adjacent/alternate channel linearity, and development of a cascaded adjacent/alternate channel analysis method.

ACKNOWLEDGMENT

The first author would like to thank Mr. Jim Oakland of Motorola CSPD RF Power Hybrids for facilitating this work and Mr. Ray Vaitkus of Motorola PCRL for reviewing this paper.

REFERENCES

[1] "Cellular System - Dual-Mode Subscriber Equipment - Network Equipment Compatibility Specification," Electronic Industries Association, IS-54, pp. 2.5 -2.9, 1989.

[2] F. G. Jenks, P.D. Morgan, and C. S. Warren, "Use of Four-Level Phase Modulation for Digital Mobile Radio," vol. EMC-14, no. 4, pp. 113-128, November 1972.

[3] Kazuki Tateoka, *et al*, "A GaAs MCM Power Amplifier of 3.6 V Operation With High Efficiency of 49% for 0.9 GHz Digital Cellular Phone Systems," IEEE MTT-S Digest, pp. 569-572, 1994.

[4] S. Narayanan, "Transistor Distortion Analysis Using Volterra Series Representation," Bell System Technical Journal, pp. 991-1024, May-June, 1967.

[5] Robert A. Minasian, "Intermodulation Distortion Analysis of MESFET Amplifiers Using the Volterra Series Representation," IEEE Transactions on Microwave Theory and Techniques, vol. MTT-28, no. 1, pp. 1-8, January 1980.

[6] Stephen A. Maas, Bradford L. Nelson, and Donald L. Tait, "Intermodulation in Heterojunction Bipolar Transistors," IEEE Transactions on Microwave Theory and Techniques, vol. MTT-40, no. 3, pp. 442-447, March 1992.

[7] Stephen A. Maas, Nonlinear Microwave Circuits, Norwood, MA: Artech House, 1988.

[8] *Mathematica Users Guide*, Wolfram Research, Inc., Champaign, IL

[9] *Hewlett-Packard Microwave Design System*, Hewlett-Packard Company, Santa Rosa, CA

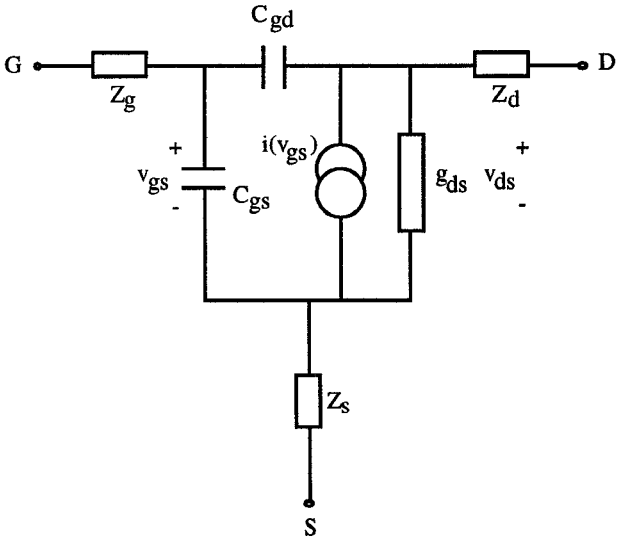

Figure 1. Simplified Extrinsic GaAs MESFET Model Used in Analysis

Table 1. Adjacent Channel Power Ratios for Each Nonlinearity

Nonlinear Parameter	g_m	C_{gs}	C_{gd}	g_{ds}
Adjacent Channel Power	-26.0 dBc	-30.1 dBc	-38.4 dBc	-39.1 dBc

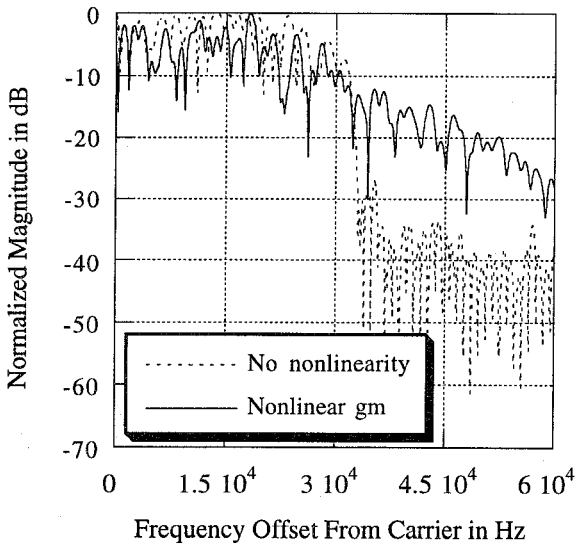

Figure 2. Spectrum Regeneration Due to Nonlinear g_m

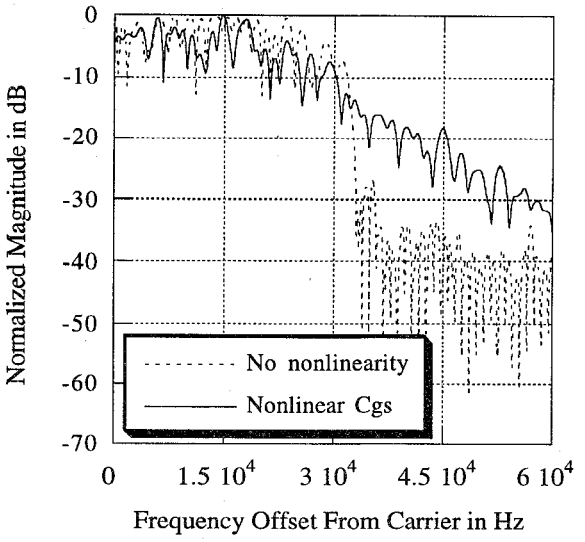

Figure 3. Spectrum Regeneration Due to Nonlinear C_{gs}

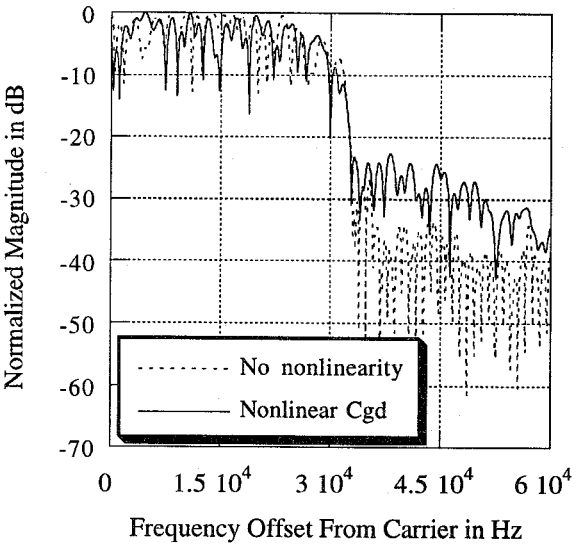

Figure 4. Spectrum Regeneration Due to Nonlinear C_{gd}

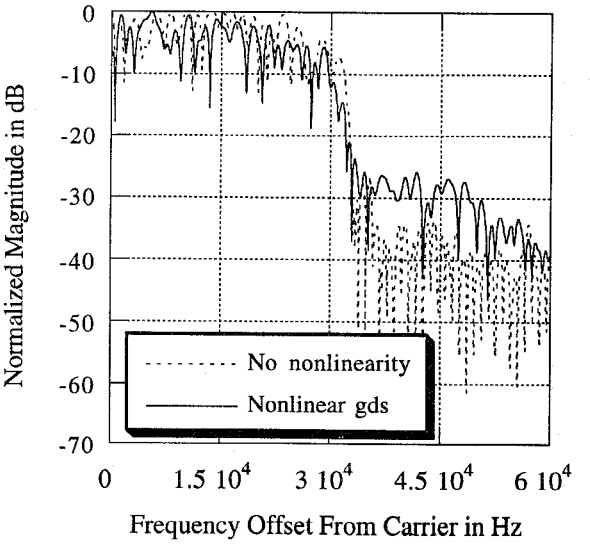

Figure 5. Spectrum Regeneration Due to Nonlinear g_{ds}